

Model and application of bidirectional pedestrian flows at signalized crosswalks

Tao Zhang(张涛), Gang Ren(任刚), Zhi-Gang Yu(俞志钢), Yang Yang(杨阳)

Citation: Chin. Phys. B . 2018, 27(7): 078901. **doi:** 10.1088/1674-1056/27/7/078901

Journal homepage: http://cpb.iphy.ac.cn; http://iopscience.iop.org/cpb

What follows is a list of articles you may be interested in

Effects of rainy weather on traffic accidents of a freeway using cellular automata model

Ming-Bao Pang(庞明宝), Bo-Ning Ren(任泊宁)

Chin. Phys. B . 2017, 26(10): 108901. **doi:** 10.1088/1674-1056/26/10/108901

Analysis of dynamic features in intersecting pedestrian flows

Hai-Rong Dong(董海荣), Qi Meng(孟琦), Xiu-Ming Yao(姚秀明), Xiao-Xia Yang(杨晓霞), Qian-Ling Wang(王千龄)

Chin. Phys. B . 2017, 26(9): 098902. **doi:** 10.1088/1674-1056/26/9/098902

A new traffic model on compulsive lane-changing caused by off-ramp

Xiao-He Liu(刘小禾), Hung-Tang Ko(柯鸿堂), Ming-Min Guo(郭明旻), Zheng Wu(吴正)

Chin. Phys. B . 2016, 25(4): 048901. **doi:** 10.1088/1674-1056/25/4/048901

A new traffic model with a lane-changing viscosity term

Ko Hung-Tang, Liu Xiao-He, Guo Ming-Min, Wu Zheng

Chin. Phys. B . 2015, 24(9): 098901. **doi:** 10.1088/1674-1056/24/9/098901

Modeling walking behavior of pedestrian groups with floor field cellular automaton approach

Lu Li-Li, Ren Gang, Wang Wei, Wang Yi

Chin. Phys. B . 2014, 23(8): 088901. **doi:** 10.1088/1674-1056/23/8/088901

Model and application of bidirectional pedestrian flows at signalized crosswalks*

Tao Zhang(张涛), Gang Ren(任刚)†, Zhi-Gang Yu(俞志钢), and Yang Yang(杨阳)

Jiangsu Key Laboratory of Urban ITS, Southeast University, Nanjing 210096, *China*

(Received 4 January 2018; revised manuscript received 20 March 2018; published online 25 June 2018)

This research of bidirectional pedestrian flows at signalized crosswalks is divided into two parts: model and application. In the model part, a mixed survey including the questionnaire investigation and tracking investigation is conducted to gain the basic data about walking tendentiousness of a pedestrian crossing. Then, the forward, right-hand, outstripping, and influential coefficients are outlined to quantize walking tendentiousness of pedestrian crossing and estimate transition probabilities of pedestrians. At last, an improved cellular automation model is proposed to describe walking tendentiousness and crossing behaviors of pedestrians. In the application part, channelization research of bidirectional pedestrian flows is presented for real signalized crosswalk. In this process, the effects of right-side-walking and conformity behaviors on the efficiency of pedestrian crossing are thoroughly analyzed based on simulations and experiments to obtain a final channelization method to raise the efficiency of a pedestrian crossing at the crosswalk.

Keywords: pedestrian flows, right-side-walking behavior, conformity behavior, simulation

PACS: 89.40.Bb, 05.50.+q, 02.50.Fz **DOI:** 10.1088/1674-1056/27/7/078901

1. Introduction

As an important pedestrian facility, the signalized crosswalk plays a pivotal role in satisfying the growing needs of pedestrians, where the pedestrian flow has the unique characteristics that should be taken into account to provide better channelization designs. At a signalized crosswalk, a platoon of pedestrians assemble at each side during the red light interval and then walk in groups to cross the street when the pedestrian light turns green. The two opposing pedestrian flows may encounter each other somewhere along the crosswalk and interact for a short period, and this interaction results in a reduction of the overall average walking speed and an increase of the total crossing time. Hence, the attention of traffic engineers should be paid to pedestrian crossing behaviors to improve the crossing efficiency of pedestrians at signalized crosswalks.

The research of pedestrian flow at signalized crosswalks is very similar to that of pedestrian counter flow, which has been studied widely by many researchers.[1–10] However, most of them simply consider the characteristics of walking tendentiousness of a pedestrian crossing, such as forward movement (i.e., the tendency to walk forward), outstripping (i.e., the tendency to outstrip another pedestrian in front), and switching lanes behaviors. Recently, some researchers have begun to describe complex characteristics of walking tendentiousness of pedestrian crossing, such as the right-side-walking (i.e., the tendency to walk right)[11–13] and conformity (i.e., when more than three same-direction people get together, a pedestrian will feel safe in the platoon, and then walk together with them)[14–16] behaviors of pedestrians, but there has been no mixed consideration of right-side-walking and conformity behaviors of pedestrians. Furthermore, in some pedestrian simulation models, although the setting of visual fields of pedestrians has been more and more accorded with the truth,[11–13,17] there has been none to distinguish different visual fields of pedestrians at different positions of signalized crosswalks. In addition, few researchers specifically modeled a pedestrian flow at the signalized crosswalks, and then made actual and detailed applied studies. Hence, here we try to overcome these shortcomings.

This paper aims to improve the crossing efficiency of pedestrians at the signalized crosswalks. A survey method includes a questionnaire investigation and tracking investigation, and involves twelve different scenes, which are utilized to identify simple and complex walking tendentiousnesses of pedestrians. A new setting of visual fields of pedestrians is proposed to depict more realistically the complex walking tendentiousness of pedestrians at the signalized crosswalks. Furthermore, the advanced definitions of transition probabilities of pedestrians are used to quantize the walking tendentiousness of a pedestrian crossing, where the forward, right-hand, outstripping, and influential coefficients are outlined to reflect the degrees of different walking tendentiousnesses of pedestrians. Based on the existing cellular automation (CA) models of pedestrian flows, we propose and analyze an improved CA model of bidirectional pedestrian flows to describe crossing behaviors of pedestrians, where walking tendentiousness is represented by the transition probabilities of pedestrians mentioned above. At last, an actually applied study is conducted

*Project supported by the National Natural Science Foundation of China (Grant No. 51578149).

†Corresponding author. E-mail: rengang@seu.edu.cn

© 2018 Chinese Physical Society and IOP Publishing Ltd

according to the proposed CA model, where channelization research of bidirectional pedestrian flow is presented to improve the crossing efficiency of pedestrians through altering the degrees of right-side-walking and conformity behaviors of pedestrians at a real signalized crosswalk.

2. Relevant literature

The main research content of this study includes model and application of bidirectional pedestrian flows at signalized crosswalks. The literature review is divided into two parts, the review of simulation models and review of applications of a pedestrian crossing.

2.1. Simulation models

Simulation is a flexible and practical method to study characteristics and dynamics of pedestrian flows. Recently, various pedestrian models have been proposed by researchers in various fields, such as agent-based,[18,19] gas kinetic,[7,17,20] social force,[21–25] and CA[2,11–14,26–29] models. However, the social force and CA models are the most well-known.

The social force concept of pedestrian flow modeling was proposed primarily by Helbing[21] and was experimentally calibrated and validated by Johansson *et al.*[22] The social force model can model the movement of each individual, which is governed by the sum of different social forces (i.e., repulsion from obstacles to individual and acting forces among individuals). However, the social forces are controlled by differential equations, whose calculation methods are complicated and immature. Therefore, this model can hardly describe some complex psychological activities of pedestrians, such as a hybrid description of right-side-walking and conformity behaviors of pedestrians.

The ability to generate fundamental pedestrian flows was demonstrated by Blue and Adler using a CA microsimulation of a pedestrian walkway with the unidirectional flow,[30] wherein six basic rules directly describe the basic forward movement and switching lanes behaviors. Then, Blue and Adler proposed a bi-directional pedestrian flow model.[31] The effort of a CA simulation related to the pedestrian counter flow was criticized and expanded upon by many other researchers.[2,11–14,32–37] The cellular-based models are simple to develop and have been proved capable of describing pedestrian movement realistically and reproducing a variety of dynamic pedestrian phenomena. Furthermore, the CA has high performance because of its simple updating rules. Hence, the pedestrian flow is modeled on the basis of a set of governing rules that can be easily modified according to the considered model reflecting various interaction rules among pedestrians. In practice, realistic modeling of the interaction between pedestrians is fundamental and critical for a reliable CA model.

However, many CA models use a set of rules to describe how pedestrian behavior is influenced by pedestrian interaction, but the rules reported by most researchers are largely dependent on certain assumptions and theories. Namely, it is unrealistic to assume an identical influence of neighbors located at different distances or directions on the focal pedestrian. This paper fills mentioned shortage, which introduces the forward, right-hand, outstripping, and influential coefficients to quantify the degrees of pedestrians walking tendentiousness according to the actual survey data (related to the pedestrians walking tendentiousness) in the definition of transition probabilities.

2.2. Application of pedestrian crossing

The modeling of a bidirectional pedestrian flow at signalized crosswalks is very different from simulations of other pedestrian flows. Namely, estimations of pedestrian crossing time and delay at signalized crosswalks require a sophisticated simulation model. To model the pedestrian flow at signalized crosswalks, Lam *et al.* studied the pedestrian walking speed–flow relationship at signalized crosswalks for different land uses.[38] Then, Lee *et al.* presented a calibration of a pedestrian simulation model based on the observation survey,[39] and Lee and Lam proposed a new pedestrian simulation model for signalized crosswalks in Hong Kong.[40] Furthermore, they also presented a further study on the development of the pedestrian simulation model at signalized crosswalks. In recent years, various kinds of pedestrian models for signalized crosswalks have been developed and proposed by many researchers from different fields.[40–44]

However, most of the simulation models related to pedestrian crossing are still in the theoretical research stage, and fewer application studies of signalized crosswalks are mainly focused on signal timing and turning lanes,[34,45] rather than to raise pedestrian crossing efficiency. Therefore, here we are trying to describe the effects of right-side-walking and conformity behaviors of pedestrians on the crossing efficiency of pedestrians and obtaining a finial channelization method based on the analysis of simulations and experiments at a real signalized crosswalk.

3. Proposed model

The model derivation is based on different walking tendentiousnesses and existing CA simulation models of pedestrians. The basic modeling process mainly includes four aspects as follows. Firstly, a mixed survey including questionnaire investigation and video tracking investigation is conducted to study the characteristics of walking tendentiousness

of pedestrian crossings using twelve kinds of different scenes. Secondly, visual fields of pedestrians are redefined to better describe different right-side-walking and conformity behaviors of pedestrians at signalized crosswalks. Then, the degrees of walking tendentiousness of pedestrian crossings are reflected by forward, right-hand, outstripping, and influential coefficients, which are outlined using the survey data in an advanced definition of transition probabilities. Finally, according to the CA pedestrian simulation model reported by Blue and Adler,[30,31] a simple set of rules, well suited in the simulation on digital computers, is made to investigate bidirectional pedestrian flow at signalized crosswalks.

3.1. Characteristics of walking tendentiousness

The walking tendentiousness of a pedestrian crossing is generally quantized by probabilities of pedestrians walking in different directions (i.e., their transition probabilities), and can characterize psychological activities of pedestrians including forward movement, outstripping, right-side-walking, and conformity behaviors. To better describe the walking tendentiousness of pedestrians (i.e., the site pedestrians select in the next step), twelve kinds of scenes are designed in Fig. 1. In the figure, the light blue square block represents the participator of a survey, the navy blue circular shape represents pedestrians regardless of the walking direction in the CA neighborhood, the red triangle that points to the right represents pedestrians walking in the same direction as the participator, and the green triangle that points to the left represents pedestrians walking in the opposite direction to the participator.

In different scenes, the CA neighborhood including five positions marked by numbers 1–5 (each position is a neighboring cell) is able to account the forward movement, switching of adjacent lanes (i.e., outstripping other pedestrians, right-side-walking, and conformity behaviors), and waiting *in situ*. Here, we do not consider the backward movement (i.e., the tendency to walk backward) because of its rarity in a pedestrian crossing. Each participator can just choose a position marked by a certain number. To acquire the site selection of pedestrians in the next step, five possible moving directions of each pedestrian are specified as forward (number 1), left (number 2), right (number 3), front left (number 4), and front right (number 5).

Purposes of twelve kinds of scenes are as follows.

Scene *a* judges pedestrian proclivities to walk in different directions.

Scene *b* obtains the right-side-walking behavior of pedestrians and judges pedestrian proclivities to outstrip another pedestrian.

Scene *c* judges pedestrian proclivities to outstrip another pedestrian.

Scene *d* obtains the right-side-walking behavior of pedestrians.

Scenes *e*–*l* describe different conformity behaviors of pedestrians under the influence of their right-side-walking behavior in various scenes.

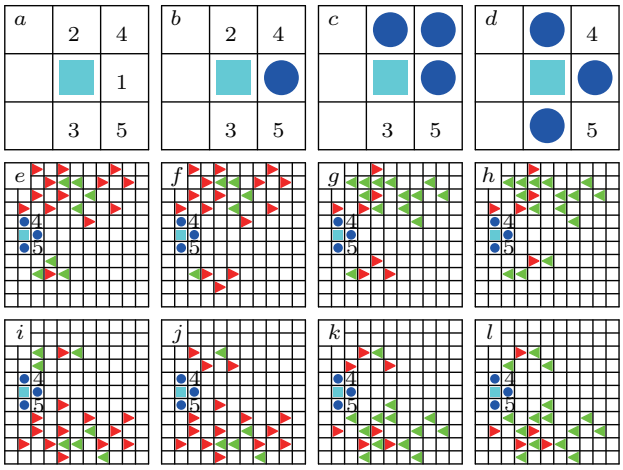


Fig. 1. (color online) Twelve kinds of scenes in the questionnaire survey.

Regarding the data collection, video tracking is a widely accepted and efficient investigation method, but it is not able to simultaneously obtain the walking tendentiousness of pedestrians in twelve kinds of scenes via pedestrian tracking, and it is hard to get the psychological activities of pedestrians in some scenes presented in Fig. 1. On the other hand, the questionnaire is inaccurate, but it can overcome disadvantages of video tracking and thoroughly obtain different walking tendentiousnesses of pedestrians at different scenes. Therefore, a mixed survey including both questionnaire investigation and video tracking investigation is designed and conducted according to the research needs.

In Chongqing of China, the pedestrians (near main road intersections, metro stations, bus stations, and railway stations) and students of Chong Qing Normal University participated in the questionnaire investigation, and they were asked to assume that they were crossing a signalized crosswalk with the high-volume pedestrian flow. Lastly, 897 questionnaires were valid. In the video tracking investigation, five videos of signalized crosswalks were shot in Nanjing and Chongqing of China, and the walk tracks of 500 pedestrians who were crossing the road were observed. Moreover, their walking tendentiousness at different scenes was recorded. The integrated results (averaged results of two investigations) are given in Table 1, where each result represents the probability that pedestrians who choose a site (i.e., a neighboring cell) in the next step are in the related scene. These results indicate that pedestrians have a powerful propensity for walking towards a destination (forward and outstripping) and are rather partial to go right. Furthermore, the right-side-walking and conformity behaviors of respondents have a certain impact on each other.

Table 1. Statistical results (%).

Scene label	Number 1 (front)	Number 2 (left)	Number 3 (right)	Number 4 (front left)	Number 5 (front right)
a	81.65	2.63	3.59	4.87	7.27
b	0	4.73	7.53	36.10	51.64
c	0	0	10.48	0	89.52
d	0	0	0	41.27	58.73
e	0	0	0	55.65	44.35
f	0	0	0	34.32	65.68
g	0	0	0	3.50	96.50
h	0	0	0	9.95	90.05
i	0	0	0	43.12	56.88
j	0	0	0	62.61	37.39
k	0	0	0	94.40	5.60
l	0	0	0	88.58	11.42

3.2. Visual field

Defining the visual field of pedestrians plays an important role in distinguishing different right-side-walking and conformity behaviors of pedestrians because different numbers of pedestrians near a certain pedestrian may influence him to have different right-side-walking and conformity behaviors. In previous studies, most researchers thought that the visual field of each pedestrian are almost the same. However, as a pedestrian gets closer to the boundary of the signalized crosswalk, his visual field is smaller than that when he is in the middle of the crosswalk (i.e., he pays more attention to what is outside of the crosswalk). Therefore, a new delimitation of visual fields of pedestrians at signalized crosswalks is proposed as follows.

Visual fields of pedestrians at different positions on a crosswalk are shown in Fig. 2, where the width of the visual field of a pedestrian decreases with the reduction of the distance between pedestrian and end side of the crosswalk. When a pedestrian is very close to his destination (i.e., the opposite side of a crosswalk), the length of his visual field is equal to the distance between a pedestrian and his destination. To distinguish different right-side-walking and conformity behaviors of pedestrians, the visual field of each pedestrian is divided into three parts: forward, left, and right. The number and proportion of other pedestrians walking in the same (or opposite) direction in left and right visual fields can describe the conformity behavior of pedestrians under the influence of their right-side-walking behavior, which can be reflected in scenes *e*–*l* in Fig. 1.

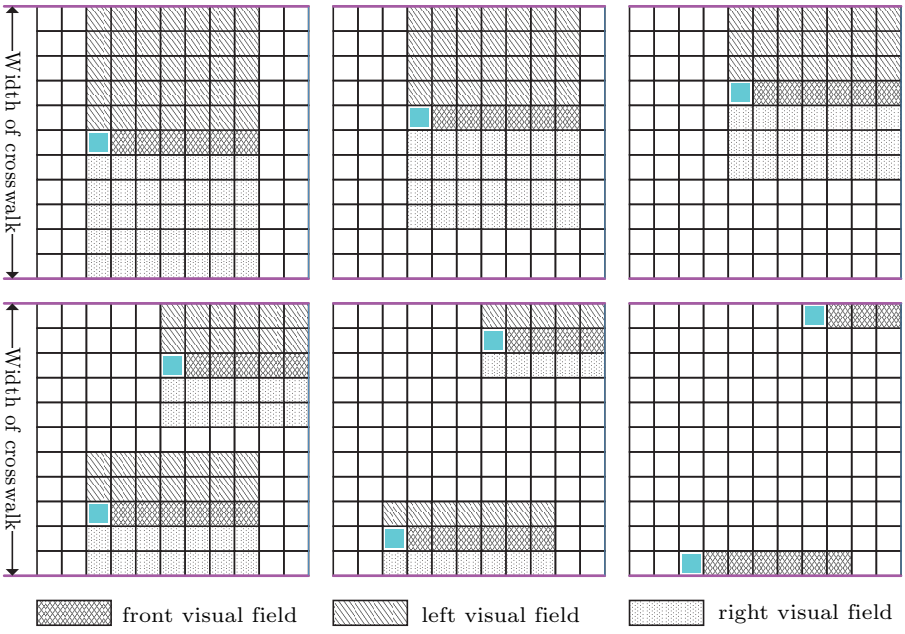


Fig. 2. (color online) Visual fields of pedestrians at different positions.

3.3. Transition probability formulation

In this section, each pedestrian can choose any unoccupied neighboring cell (but only one) with a certain probability, or stays at the original position if all neighboring cells are occupied by other pedestrians in that time step. The corresponding diagram is shown in Fig. 3, where P_m ($m = 1, 2, 3, 4, 5$) is the transition probability of the corresponding position (neighboring cell) selected by a pedestrian.

When walking tendentiousness of pedestrians is not considered, each pedestrian has an initial transition probability p_0 of each cell in the CA neighborhood defined as

$$p_0 = \begin{cases} 0, & \text{the cell is occupied,} \\ 1/n, & \text{the cell is free,} \end{cases} \tag{1}$$

where n is the number of unoccupied neighboring cells.

However, in order to simulate a bidirectional pedestrian flow at the signalized crosswalk better, the forward, right-hand, outstripping, and influential coefficients are quoted to quantize different walking tendentiousnesses of pedestrians, then to correct the initial transition probability. The forward,

right-hand, and outstripping coefficients have been involved by Yue *et al.*[11,12] and Ren *et al.*[13] to describe forward movement, right-side-walking, and outstripping behaviors, while the influential coefficients are here proposed for the first time to depict the conformity behavior under the influence of right-side-walking behavior of pedestrians.

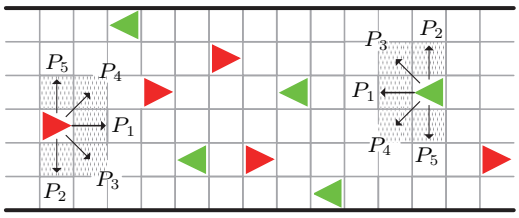


Fig. 3. (color online) Diagram of transition probability of pedestrians.

3.3.1. First correctional transition probability

The forward movement, outstripping, and right-side-walking behaviors are first quantized by

$$\begin{cases} f = (N_{a1}/N_{a2} + N_{a1}/N_{a3} + N_{a1}/N_{a4} + N_{a1}/N_{a5})/4, \\ r = [(N_{b3} + N_{b5})/(N_{b2} + N_{b4}) + N_{\mathrm{d}5}/N_{\mathrm{d}4}]/2, \\ s = [(N_{b4} + N_{b5})/(N_{b2} + N_{b3}) + N_{c5}/N_{c3}]/2, \end{cases} \tag{2}$$

where f is forward coefficient, r is right-hand coefficient, s is outstripping coefficient, N_{a1} (71.46%) is the probability of participators to choose the neighboring cell marked by a number 1 in scene a, which is listed in Table 1. The notation N_{a1} is similar in meaning to notations N_{a2} (4.24%), N_{b2} (7.27%), N_{c3} (19.02%), etc. Likewise, the definitions of these notations are equally applied to Eq. (4). Taking data from Table 1 into Eqs. (2) and (4) can make our survey determine the relevant coefficients, and thereby impact our model.

Then, the initial transition probability of each neighboring cell is corrected by

$$\begin{aligned} &P_1 = fp_0, \quad P_2 = rp_0, \quad P_3 = srp_0, \\ &P_4 = sp_0, \quad P_5 = p_0. \end{aligned} \tag{3}$$

This corrected transition probability is called the first correctional transition probability, and it is applicable to the pedestrians in whose right and left visual fields there is no other pedestrian.

3.3.2. Second correctional transition probability

According to Fig. 1 and Table 1, there are two resemblances in both scenes e and f. On the one hand, the number of pedestrians in the left visual field of the pedestrian is bigger than that in the right visual field. In addition, the number of pedestrians walking in the same direction in the left visual pedestrian field is higher than that in the right one. On the other hand, the percentages of pedestrians that walk right are similar in both scenes. Hence, the same influential coefficient is used in both scenes e and f. In that manner, influence coefficients are determined in scenes g–l. Then, four kinds of scenes (i.e., scenes e and f, g and h, i and j, k and l) are recombined to show different effects of conformity behavior on right-side-walking behavior.

The conformity behavior under the influence of right-side-walking behavior is quantized to influential coefficients given by

$$\begin{cases} cr1 = (N_{e5} + N_{f5})/(2N_{\mathrm{d}5}), cl1 = (N_{e4} + N_{f4})/(2N_{\mathrm{d}4}), \\ cr2 = (N_{g5} + N_{h5})/(2N_{\mathrm{d}5}), cl2 = (N_{g4} + N_{h4})/(2N_{\mathrm{d}4}), \\ cr3 = (N_{i5} + N_{j5})/(2N_{\mathrm{d}5}), cl3 = (N_{i4} + N_{j4})/(2N_{\mathrm{d}4}), \\ cr4 = (N_{k5} + N_{l5})/(2N_{\mathrm{d}5}), cl4 = (N_{k4} + N_{l4})/(2N_{\mathrm{d}4}), \end{cases} \tag{4}$$

where $cl1$ and $cr1$ are the left and right influential coefficients in scenes e and f, respectively. $cl1$ and $cr1$ are similar in meaning to cl 2 and $cr2$ (in scenes g and h), $cl3$ and $cr3$ (in scenes i and j), and $cl4$ and $cr4$ (in scenes k and l).

Then, the initial transition probability of each neighboring cell is corrected by

$$\begin{cases} P_1 = fp_0, \quad P_2 = crirp_0, \\ P_3 = crisrp_0, \quad P_4 = clisp_0, \\ P_5 = clip_0, \quad i = 1,2,3,4. \end{cases} \tag{5}$$

The corrected transition probability is the second correctional transition probability, which is applicable to the pedestrians in whose right and left visual fields there are one or more pedestrians.

Results of relevant coefficients from Table 2 are calculated respectively using survey data in Table 1 and Eqs. (2) and (4).

Table 2. Calculated values of relevant coefficients.

Symbol	Name	Value
f	forward coefficient	20.46
r	right-hand coefficient	1.44
s	outstripping coefficient	7.85
$cr1$	right influential coefficient of scenes e and f	0.94
$cl1$	left influential coefficient of scenes e and f	1.09
$cr2$	right influential coefficient of scenes g and h	1.59
$cl2$	left influential coefficient of scenes g and h	0.16
$cr3$	right influential coefficient of scenes i and j	0.8
$cl3$	left influential coefficient of scenes i and j	1.28
$cr4$	right influential coefficient of scenes k and l	0.14
$cl4$	left influential coefficient of scenes k and l	2.22

3.3.3. Disposed transition probability

After the first and second correctional transition probabilities are calculated by Eqs. (3) and (5) respectively, they need to be disposed by

$$P_{\mathrm{d}1} = P_1 / \sum_{m=1}^{5} P_m, \quad P_{\mathrm{d}2} = P_2 / \sum_{m=1}^{5} P_m, \quad P_{\mathrm{d}3} = P_3 / \sum_{m=1}^{5} P_m$$

$$P_{d4} = P_4 / \sum_{m=1}^{5} P_m, \quad P_{d5} = P_5 / \sum_{m=1}^{5} P_m, \tag{6}$$

where P_{d1} denotes the disposed transition probability of P_1. P_{d1} is similar in meaning to P_{d2}, P_{d3}, P_{d4}, and P_{d5}. The disposed transition probability can be directly applied in the model formulation (Section 3.4) to determine the walking direction of pedestrians.

3.4. Model formulation

The crosswalk layout is shown in Fig. 4, where the crosswalk area is A with width W and length L, $A = W \times L$, is filled with black and white wide lines. The two gray parts are the waiting area of pedestrians. When the signal light is red, pedestrians have to wait for a green light on waiting areas. The two pink parts are the extension areas ($w \times L$). In reality, pedestrians may walk out of the crosswalk (i.e., illegal crossing) to mitigate conflicts with other pedestrians.

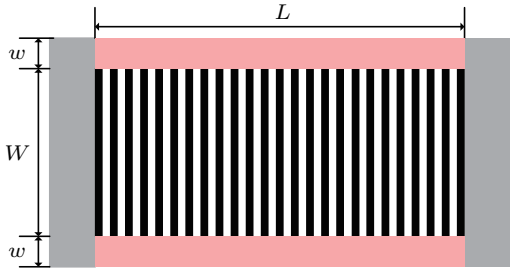


Fig. 4. (color online) Illustration of signalized crosswalk.

The presented layout is closed and enables pedestrians to interact while maintaining strict conservation of the flow. Each cell (position) is either free or occupied by a certain pedestrian. At the start of each simulation, the imaginary density ID (ID = all pedestrians passing the crosswalk/total number of cells within area A) is between 0.05 and 1.0, which remains constant in each run. The number of pedestrians who are created and assigned to waiting areas at the start of each simulation is $N_{ped} = \text{INT}(ID \times A)$, where INT denotes the rounding functionality. The total simulation time represents the period between the moment when the first pedestrian enters the crosswalk and the moment when the last pedestrian leaves the crosswalk. A time step is 1 second (s).

Blue and Adler[30,31] built a set of CA rules for pedestrian flow, which were approved and used by many researchers. Here, we improve their rules for bidirectional pedestrian flow at signalized crosswalks, and the main improvements are as follows.

i) In addition to the forward movement, switching adjacent lanes, and waiting *in situ*, there are two extra fundamental elements of pedestrian movement that are taken into account: exchanging position and conflict resolution. Exchanging position and conflict resolution are able to avoid the head-on deadlock and cell shared by several pedestrians, respectively.

ii) In order to check whether counter flows are affected by right-side-walking and conformity behaviors of pedestrians, the definition of "opposite conflict state" is proposed. Namely, if one or more opposite pedestrians are found in the right and left visual fields of a pedestrian, he is supposed to be in an opposite conflict state. Two different types of states should be distinguished: unidirectional conflict and opposite conflict states.

In the unidirectional conflict state, the first correctional transition probability is disposed, which is similar to that reported by Yue *et al.*[11,12] and Ren *et al.*[13]

In the opposite conflict state, the second correctional transition probability is disposed, which appropriately refers to right-side-walking and conformity behaviors of pedestrians in different scenes in Fig. 1.

iii) The illegal behavior of pedestrian crossing is considered, which makes a pedestrian gain health and environmental benefits (i.e., faster and more comfortably crossing) by minimizing the associated risks.[46] The behavior is represented by a rule which defines that each pedestrian (at the crosswalk area and near the extension areas) walks to the extension area with a certain probability, and then allocates a suitable velocity to walk forward in the area. We assume that the pedestrian in the extension areas is not able to return to the crosswalk area.

4. Analysis

4.1. Simulations

The model described above was executed on a crosswalk ($L = 50$ cells, $W = 12$ cells, and $w = 2$ cells) according to the recommendation of standards and regulations in China. Each cell was considered as a square with a side of 0.4 meter (m), which was scaled based on the minimal requirements for personal space in China. According to the Highway Capacity Manual (HCM),[47] three kinds of velocities (0.8 m/s, 1.2 m/s, and 1.6 m/s) were selected and randomly applied using the ration 5/75/20 in the first row of waiting pedestrians who were assumed to be at the unsignalized intersection. Two values of velocities (1.2 m/s and 1.6 m/s) were selected and randomly applied using the ration 80/20 by pedestrians (in the extension areas) who had illegally crossed. The maximum and minimum speeds of other pedestrians were 1.2 m/s and 0.4 m/s, respectively. Moreover, the delay was emphasized during the simulations. If two opposite pedestrians were head-on and adjacent, a delay occurred between them (even delay time of 0.2 s was brought).[14] Note that a pedestrian may cause one or more delays during the crossing process.

In the simulation, three fundamental parameters were observed. The crossing time (CT) was defined as the number of time steps of pedestrians taken in simulation and their delay times. The mean crossing speed (MCS) and mean pedestrian

delay (*MPD*) were the average speed and delay of all pedestrians passing the crosswalk, respectively. Results of *CT*, *MCS*, and *MPD* were computed by

$$\begin{cases} CT = \max\limits_{j=1,2,\ldots,N_{\text{ped}}} \{t_j + 0.2n_j\}, \\ MCS = \sum\limits_{j=1}^{N_{\text{ped}}} [0.4L/(t_j + 0.2n_j)]/N_{\text{ped}}, \\ MPD = \sum\limits_{j=1}^{N_{\text{ped}}} (0.2n_j)/N_{\text{ped}}, \end{cases} \tag{7}$$

where t_j is the time that the pedestrian j needed to pass the crosswalk, and n_j is the number of delays of pedestrian j.

To generate fundamental parameters of pedestrian flow, the simulations were conducted with different imaginary densities (*ID*s) ranging from 5% to 95% cell occupancy with the step of 5%. The pedestrians were randomly assigned to both waiting areas with ten percent split in walking direction (90/10, 80/20, 70/30, 60/40, 50/50). Each simulation was run for 50 times, and the simulation results were averaged.

4.2. Model validation

The proposed model was validated by analysis of *MCS*–*ID* curves, comparison of *CT*–*ID* curves between simulations and other credible merits, and the research of pedestrian distribution.

Figure 5 depicts results of simulations conducted over a range of directional split increment of 10% from 90/10 to 50/50. As expected, simulation results in terms of *MCS* correspond to "well-established level-of-service criteria" (3.0–3.5 ft/s) defined in Chapter 4 in the HCM[47] for a low density, and they are in excellent agreement with the field data in a high-density condition.

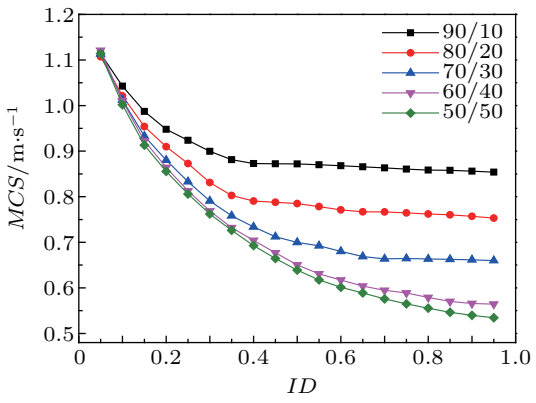


Fig. 5. (color online) The *MCS*–*ID* curves of bidirectional pedestrian flow for different splits.

Simulation results in terms of *CT* were compared with two empirical models proposed by Golani and Damti[48] with different *ID*s for 90/10 and 50/50 directional splits, since these two directional splits are very common in real life. Both empirical models were calibrated with the significant amount of observation data, and have been proven to be solid via engineering practices. In some sense, comparisons with both models were similar to comparisons with real field data indirectly. Figure 6 illustrates that three lines match quite well when *ID* is less (less than 0.1). However, as *ID* increases, *CT* values of model 1 are much higher than those of the proposed model and model 2, which is consistent with the finding by Golani and Damti that model 1 is suitable only for low volume.[48] In addition, it was found that the *CT*–*ID* curve of this model was identical to that of model 2 in Fig. 6(a). However, as it can be seen in Fig. 6(b), the results of *CT* are slightly shorter than those of model 2, which is caused by the different arrival rates of pedestrians. Consequently, the proposed model can accurately estimate the *CT*.

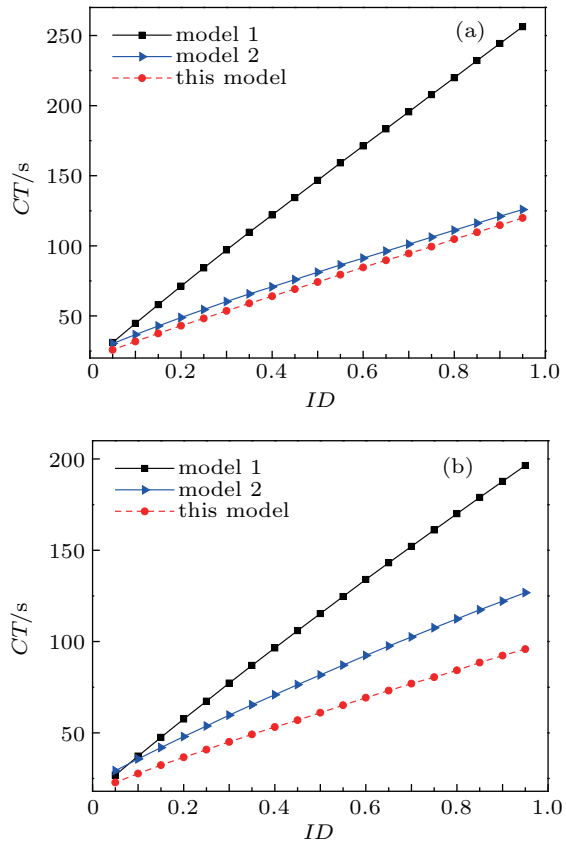


Fig. 6. (color online) Comparisons of crossing time between this model and two common empirical models for (a) 90/10 and (b) 50/50 directional splits.

Figure 7 shows the distribution of pedestrians for *ID* of 0.5 for 50/50 directional split on the crosswalk for different time steps. This graphic is a perfect illustration of pedestrian crossing (time step = 5 s, 15 s, 25 s, and 50 s), which reveals well the right-side-walking and conformity behaviors of pedestrians. Therefore, during the simulation, we were capable of capturing the mental and behavioral characteristics of pedestrians, and describing the interactions among them.

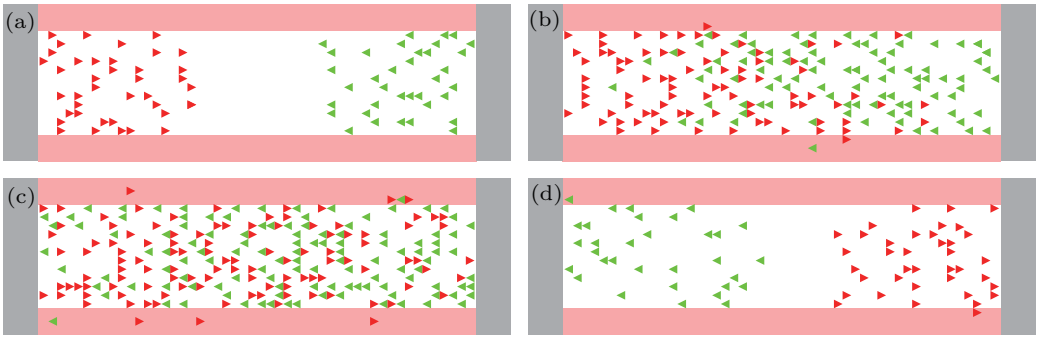


Fig. 7. (color online) Distribution of pedestrians at the crosswalk for time steps of (a) 5 s, (b) 15 s, (c) 25 s, and (d) 50 s.

5. Application

In this section, channelization research of bidirectional pedestrian flow at the signalized crosswalks using the proposed model. At first, we selected a real signalized crosswalk with the larger pedestrian flow, which was near the subway station of Chongqing of China, and about 14 m long and 7.5 m wide. Series of simulation runs were executed on a virtual crosswalk (using almost the same layout as that of the selected signalized crosswalk). The research range of *ID* of the crosswalk was determined through different curves for bidirectional pedestrian flows with various splits. Then, we studied the effects of right-side-walking and conformity behaviors on pedestrian crossing efficiency at the crosswalk and obtained a channelization suggestion (i.e., how to raise pedestrian crossing efficiency) at the crosswalk. Finally, according to the proposed channelization suggestions, real experiments were performed (as required) on the selected crosswalk. We compared experimental results with simulation results, and a new (final) channelization method of the crosswalk was determined to improve the crossing efficiency of pedestrians. The explained research process is shown in Fig. 8.

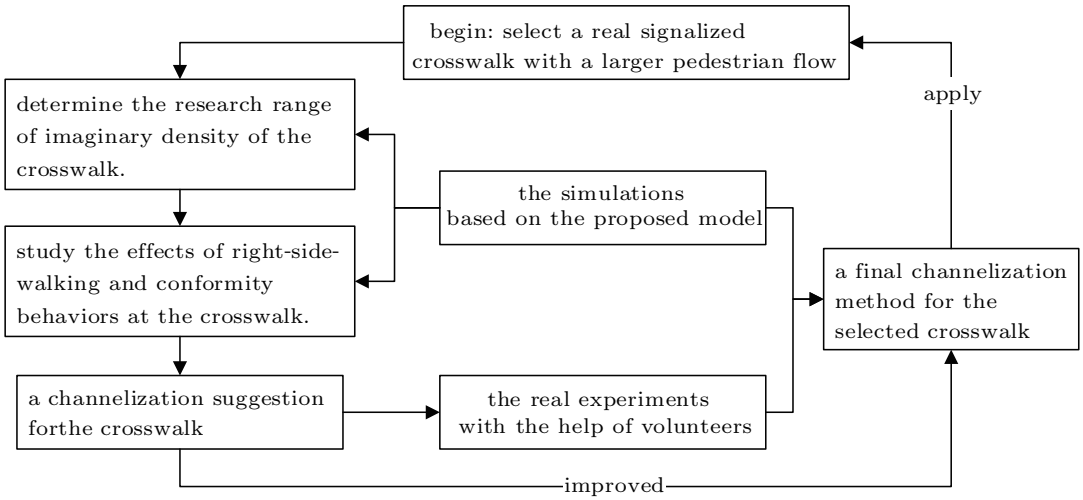


Fig. 8. Flowchart of the channelization research.

5.1. Research range of imaginary density

The research range of *ID* is important to the investigation of bidirectional pedestrian flow at signalized crosswalks, and its determination is a challenge for the computer graphics community. If the imaginary density is too small, there is no need for a study. On the other hand, if the imaginary density is too high, there is almost no such phenomenon in reality. To determine an appropriate range of selected signalized crosswalk, a series of simulations on virtual crosswalk were conducted with different *ID*s for five directional splits. The running times of simulations were the same as before, and the simulation results were also averaged.

As illustrated in Fig. 9, with the reference of Fig. 5, as directional splits change with the increment of 10% from 90/10 to 50/50, the results of *CT* and *MCS* are reducing, whereas the values of *MPD* are increasing. For *ID*s above 0.4, there is a relatively small change of *MCS* and *MPD* as *ID*s increase. Moreover, the *CT* results are greater than 40 s and do not accord with the truth. However, it was found that the region of *ID* [0.05–0.4] has the largest differences in *MCS* and *MPD* for a maximal inclined angle. However, *CT*, *MCS*, and *MPD* are within the acceptable limits of traffic planners for low *ID* [0.05–0.1). In summary, the research range of *ID* was defined

as [0.1–0.4] for selected signalized crosswalks.

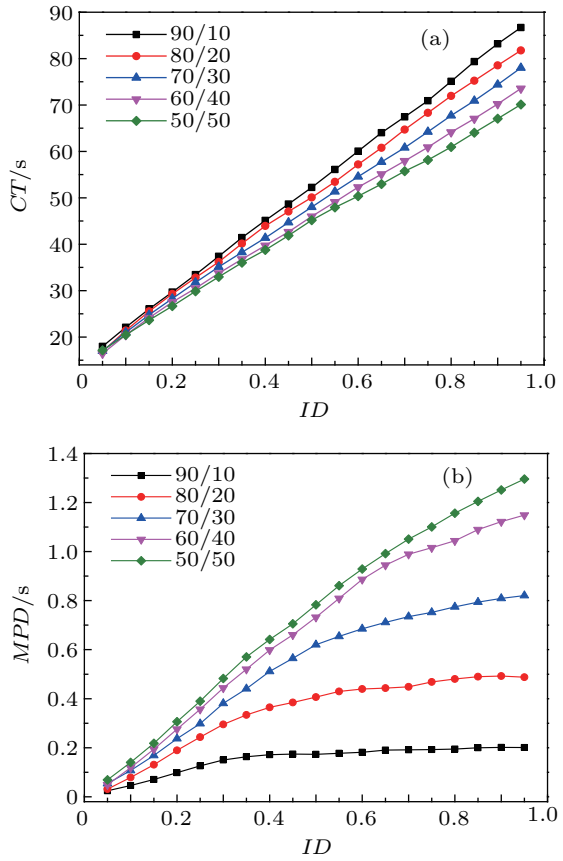


Fig. 9. (color online) Curves of bidirectional pedestrian flow for different splits. (a) The *CT–ID* curves. (b) The *MPD–ID* curves.

5.2. Effects of right-side-walking and conformity behaviors

Based on the results of the mixed survey and actual circumstances of a pedestrian crossing, it was found that right-side-walking and conformity behaviors have a great effect on properties of the pedestrian crossing and can be controlled by the subjective consciousness of pedestrians. Therefore, the behaviors of pedestrian crossing were modeled using varying survey data in the research range of *ID* [0.1–0.4] for 50/50 and 90/10 directional splits, respectively. Unlike the above simulations, these simulations run for 200 times on the virtual crosswalk to obtain more accurate results, and simulation results were averaged.

5.2.1. Degrees of right-side-walking and conformity behaviors

The right-side-walking behavior was associated with probabilities P_{b3}, P_{b5}, and P_{d5}, and the conformity behavior was associated with probabilities P_{e4}, P_{f4}, P_{i5}, and P_{j5}, according to the formulas of transition probability and data of our survey. Results of different modified coefficients were calculated using transition probability formula for varying degrees (related probabilities) of right-side-walking and conformity behaviors, respectively. The modified coefficients for different degrees of right-side-walking behavior is listed in Table 3, where R_{+10} describes a degree of right-side-walking behavior when the original probabilities (associated with right-side-walking behavior) increase by 10%. In that case, the increment of P_{d5} was 10%, whereas increments of P_{b3} (2%) and P_{b5} (8%) added up to 10% (since the value of P_{b5} was about four times greater than P_{b3} when the degree of right-side-walking behavior was R_0). In addition, R_{-10}, R_0, R_{+20}, and R_{+30} were similar in meaning to R_{+10}. In that manner, C_{-20}, C_{-10}, C_0, C_{+10}, and C_{+20} can be explained to show different degrees of conformity behavior, and they are listed in Table 4. Note that the *CT–ID* curves are not discussed in this section, because the length of *CT* is determined by the last pedestrian, and has a small influence on right-side-walking and conformity behaviors.

Table 3. Modified coefficients for different degrees of right-side-walking behavior.

Degree	Related probabilities	Modified right-hand coefficient
R_{-10}	$P_{b3} = 5.53\%$, $P_{b5} = 43.64\%$, $P_{d5} = 48.73\%$	$r = 0.96$
R_0	$P_{b3} = 7.53\%$, $P_{b5} = 51.64\%$, $P_{d5} = 58.73\%$	$r = 1.44$
R_{+10}	$P_{b3} = 9.53\%$, $P_{b5} = 59.64\%$, $P_{d5} = 68.73\%$	$r = 2.22$
R_{+20}	$P_{b3} = 11.53\%$, $P_{b5} = 67.64\%$, $P_{d5} = 78.73\%$	$r = 3.75$
R_{+30}	$P_{b3} = 13.53\%$, $P_{b5} = 75.64\%$, $P_{d5} = 88.73\%$	$r = 8.05$

Table 4. Modified coefficients for different degrees of conformity behavior.

Degree	Related probabilities	Modified influential coefficients
C_{-20}	$P_{e4} = 35.65\%$, $P_{f4} = 14.32\%$ $P_{i5} = 36.88\%$, $P_{j5} = 17.39\%$	$cr1 = 1.28$, $cl1 = 0.61$, $cr3 = 0.46$, $cl3 = 1.77$
C_{-10}	$P_{e4} = 45.65\%$, $P_{f4} = 24.32\%$ $P_{i5} = 46.88\%$, $P_{j5} = 27.39\%$	$cr1 = 1.11$, $cl1 = 0.85$, $cr3 = 0.63$, $cl3 = 1.52$
C_0	$P_{e4} = 55.65\%$, $P_{f4} = 34.32\%$ $P_{i5} = 56.88\%$, $P_{j5} = 37.39\%$	$cr1 = 0.94$, $cl1 = 1.09$, $cr3 = 0.80$, $cl3 = 1.28$
C_{+10}	$P_{e4} = 65.65\%$, $P_{f4} = 44.32\%$ $P_{i5} = 66.88\%$, $P_{j5} = 47.39\%$	$cr1 = 0.77$, $cl1 = 1.33$, $cr3 = 0.97$, $cl3 = 1.04$
C_{+20}	$P_{e4} = 75.65\%$, $P_{f4} = 54.32\%$ $P_{i5} = 76.88\%$, $P_{j5} = 57.39\%$	$cr1 = 0.60$, $cl1 = 1.57$, $cr3 = 1.14$, $cl3 = 0.80$

5.2.2. Effects of right-side-walking behavior

In Figs. 10(a) and 10(b), the values of *MPD* decrease when the degree of right-side-walking behavior increases for both 50/50 and 90/10 directional splits. These findings indicate that the enhancement of right-side-walking behavior can reduce the *MPD*. In Fig. 10(c), with the increase of degree of right-side-walking behavior for 90/10 directional split, the *MCS* gradually decreases because some pedestrians have the tendency to move diagonally with a strong right-side-walking

behavior. As shown in Fig. 10(d), for 50/50 directional split, the stronger the right-side-walking behavior is in the *ID* range of [0.1–0.15], the higher the *MCS* is. Further, the *MPD* is low within the *ID* range of [0.20–0.4]. Lastly in the interweaving area, the *ID* range of (0.15–0.20) is hard to analyze. The *MCS* increases when a degree of right-side-walking behavior increases at low *ID*s, because the reduction of *MPD* makes a bigger impact on the *MCS* than the tendency of some pedestrians to move diagonally with a strong right-side-walking behavior.

Comparing Figs. 10(a) and 10(c) with Figs. 10(b) and 10(d), we can conclude that right-side-walking behavior has a greater effect on the pedestrian crossing of balanced (approximate 50/50 directional split) flows than that of imbalanced (approximate 90/10 directional split) flows.

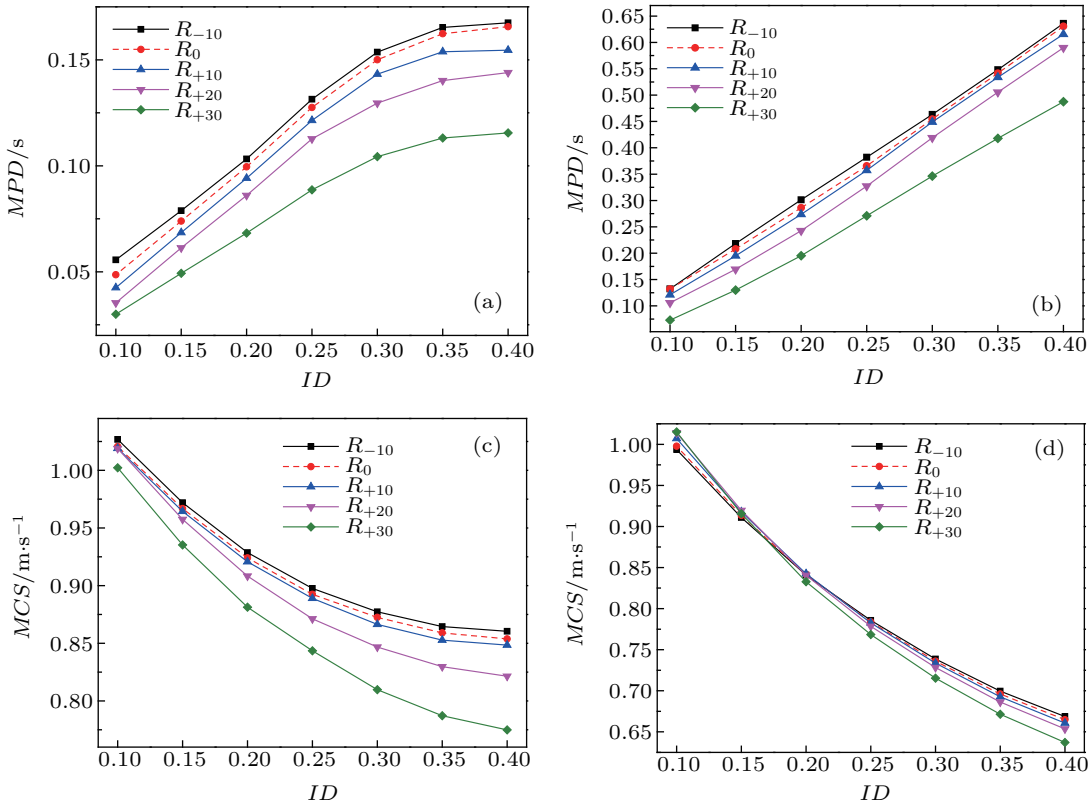


Fig. 10. (color online) Curves for different degrees of right-side-walking behavior. (a) The *MPD–ID* curves for 90/10 directional split. (b) The *MPD–ID* curves for 50/50 directional split. (c) The *MCS–ID* curves for 90/10 directional split. (d) The *MCS–ID* curves for 50/50 directional split.

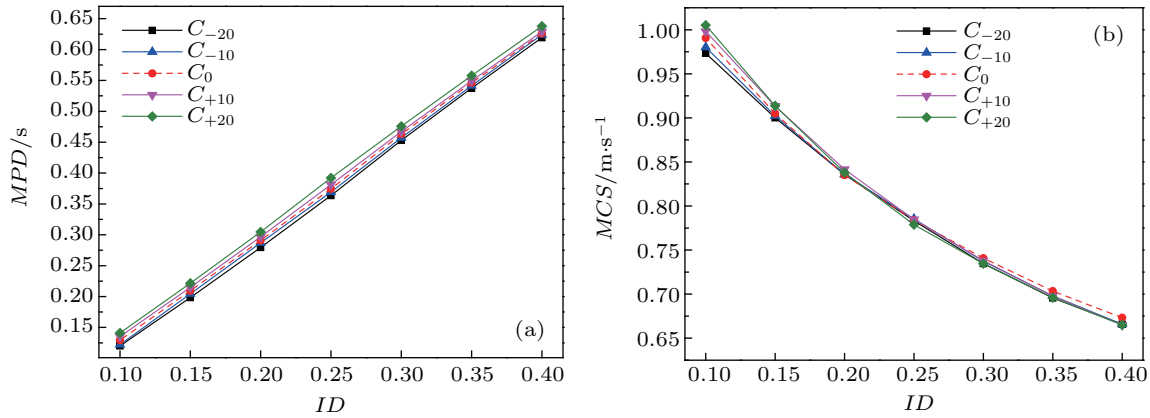


Fig. 11. (color online) Curves for different degrees of conformity behavior. (a) The *MPD–ID* curves for 50/50 directional split. (b) The *MCS–ID* curves for 50/50 directional split.

5.2.3. Effects of conformity behavior

Due to the small effect of conformity behavior on bidirectional pedestrian flow for 90/10 directional split, the balanced flow is only discussed here.

Figure 11(a) shows that *MPD* increases when the degree of conformity behavior increases for 50/50 directional split,

which implies that the enhancement of conformity behavior can have an extra delay of the pedestrian crossing. As shown in Fig. 11(b), for 50/50 directional split, the stronger the conformity behavior is within the *ID* range of [0.1–0.15], the higher the *MCS* is, because the enhancement of conformity behavior can weaken the tendency of some pedestrians to move diagonally (i.e., may weaken the degree of right-side-walking behavior). In the *ID* range of [0.25–0.4], the *MCS* decreases regardless whether the degree of conformity behavior raises or reduces, which is caused by the increase of *MPD* of pedestrian crossing with a strong conformity behavior. The *ID* range of (0.15–0.25) is not analyzed because that was an interweaving area.

Given that there is a slight variation in results among varying degrees of conformity behavior, a significant discovery is that conformity behavior has a smaller effect on pedestrian crossing than right-side-walking behavior.

5.2.4. Channelization suggestion

In view of the analysis within Sections 5.2.2 and 5.2.3, we can get a channelization suggestion that for the selected crosswalk, in the *ID* range of [0.1–0.4], by enhancing the right-side-walking behavior of pedestrians and weakening the conformity behavior of pedestrians, we can reduce *MPD* of pedestrian crossing, but pedestrians should not move diagonally to improve *MCS* of pedestrian crossing.

5.3. Channelization method

In this section, the results of real experiments conducted at the selected signalized crosswalk are compared with the simulations to obtain a final channelization method. With the reference of the channelization suggestion mentioned in Section 5.2.4, these experiments need to achieve real videos of pedestrian crossing with different degrees of right-side-walking and conformity behaviors for different directional splits in the research *ID* range of pedestrians. However, it is very difficult to make such videos at peak time at the crosswalk without the help of pedestrians. Hence, 80 volunteers who were students at Chong Qing Normal University were recruited to participate in our experiments at the selected crosswalk. Please note that participants in experiments include both random pedestrians and volunteers. The experiments were as follows.

In the case of Text 1 (i.e., a rough experiment for directional split 90/10), when the light turned green, 40 volunteers on one side of the crosswalk began to cross. On the other hand, in Text 2 (i.e., a rough experiment for the directional split 50/50), when the light turned green, 80 volunteers (averagely distributed to both waiting areas of the crosswalk) began to cross. Texts 1 and 2 were done, respectively, after volunteers had been told to try to implement the channelization suggestion. Sample photos are shown in Fig. 12.

In Fig. 12(a), the participants showed a strong conformity behavior, resulting in a phenomenon that there are few pedestrians within the red line of the crosswalk. However, such a phenomenon does not exist in Fig. 12(c), because the weakening of conformity behavior not only reduced the delay of a pedestrian crossing but also increased the utilization of the crosswalk. As expected, the efficiency of pedestrian crossing in Fig. 12(d) was higher than that in Fig. 12(b) due to the implementation of channelization suggestion.

Then, these four Tests were simulated by the proposed model, where the simulations of Figs. 12(a) and 12(b) were conducted with the original relevant coefficients, and the simulations of Figs. 12(c) and 12(d) were conducted with the modified coefficients which made the degree of right-side-walking behavior increase by 20% and the degree of conformity behavior decrease by 20%. Simulations were run 200 times, and the results were averaged. As Table 5 shows, the difference of parameters between simulations and experiments is within 20%, which is acceptable for the simulation of pedestrian motion.



Fig. 12. (color online) Photos obtained by the comparative tests. (a) The screen of Text 1. (b) The screen of Text 2. (c) The told screen of Text 1. (d) The told screen of Text 2.

Table 5. Comparison of experiments and simulations.

Text number	The number of participants at both sides of the crosswalk	*CT* of experiment and simulation/s	*MCS* of experiment and simulation/m·s^{-1}
1	51/9	25 and 22.392	0.9361 and 1.0055
2	58/52	30 and 25.722	0.8073 and 0.8644
3	54/15	25 and 22.940	0.9791 and 1.0195
4	62/50	29 and 27.036	0.9072 and 0.8739

In conclusion, the channelization suggestion can be considered as a final channelization method to promote pedestrian crossing at the selected signalized crosswalk.

6. Conclusion

The model for bidirectional pedestrian flows at the signalized crosswalks is proposed incorporating the characteristics of walking tendentiousness and CA model to describe the psychological activities and crossing behaviors of pedestrians. Compared to the other models, the proposed model not only determines the walking tendentiousness of pedestrian crossing (including forward movement, outstripping, right-side-walking, and conformity behaviors) which is obtained through the mixed survey, but also takes into account different visual fields of pedestrians at different positions, different transition probabilities at different conflict states, and illegal crossing behaviors. Moreover, the proposed model was verified by analysis of *MCS–ID* curves, a comparison of *CT–ID* curves of the model and other two empirical models, and research of pedestrian distribution in simulations.

Based on the proposed model, channelization research is presented for bidirectional pedestrian flows at a signalized crosswalk. In this process, for the crosswalk, we determine the *ID* research range of [0.1–0.4] and study the effects of right-side-walking and conformity behaviors on the efficiency of a pedestrian crossing. Finally, combining experiments and simulations, a final channelization method for crosswalk is proposed to promote pedestrian crossing.

This paper indicates that the methodology based on the combination of simulations and experiments, which denotes the channelization method, is important for the determination of pedestrian flows at signalized crosswalks and has broad application prospects for various aspects of traffic flows. In the future, in-depth studies are required to incorporate the interaction between pedestrians and vehicles into the simulation model and investigate effects of the walking tendentiousness on pedestrian crossing time, speed, and delay.

Acknowledgment

The authors are very grateful to the teachers and students at Chong Qing Normal University for their work on the questionnaire survey and real tests.

References

[1] Muramatsu M, Irie T and Nagatani T 1999 *Physica A* **267** 487
[2] Yu Y F and Song W G 2007 *Phys. Rev. E* **75** 046112
[3] Kuang H, Song T, Li X L and Dai S Q 2008 *Chin. Phys. Lett.* **25** 1498
[4] Kuang H, Li X L, Song T and Dai S Q 2008 *Phys. Rev. E* **78** 066117
[5] Kuang H, Song T, Dai S Q and Li X L 2009 *Int. J. Mod. Phys. C* **20** 1945
[6] Ma J, Song W G, Zhang J, Lo S M and Liao G X 2010 *Physica A* **389** 2101
[7] Kuang H, Li X L, Wei Y F, Song T and Dai S Q 2010 *Chin. Phys. B* **19** 070517
[8] Ma J, Song W G and Liao G X 2010 *Chin. Phys. B* **19** 128901
[9] Xiong T, Zhang P, Wong S C, Shu C W and Zhang M P 2011 *Chin. Phys. Lett.* **28** 108901
[10] Li X, Duan X Y and Dong L Y 2012 *Chin. Phys. B* **21** 108901
[11] Yue H, Shao C F, Chen X M and Hao H R 2008 *Acta Phys. Sin.* **57** 6901 (in Chinese)
[12] Yue H, Guan H Z, Zhang J and Shao C F 2010 *Physica A* **389** 527
[13] Ren G, Lu L L and Wang W 2012 *Acta Phys. Sin.* **61** 144501 (in Chinese)
[14] Zhang J, Wang H and Li P 2004 *J. Zhejiang Univ. Sci.* **5** 835
[15] Zhou R G, Horrey W and Yu R 2009 *Accid. Anal. Prev.* **41** 491
[16] Zhou R G and Horrey W 2010 *Transp. Res. Part. F* **13** 153
[17] Kuang H, Chen T, Li X L and Lo S M 2014 *Nonlinear Dyn.* **78** 1709
[18] Batty M 2001 *Environ. Plann. B Plann.* **28** 321
[19] Rindsfüser G and Klügl F 2007 *DisP-The Plan. Rev.* **43** 9
[20] Yue H, Hao H R, Chen X M and Shao C F 2007 *Physica A* **384** 567
[21] Helbing D and Molnar P 1995 *Phys. Rev. E* **51** 4282
[22] Johansson A, Helbing D and Shukla P K 2007 *Adv. Complex Syst.* **10** 271
[23] Song W G, Yu Y F, Wang B H and Fan W C 2006 *Physica A* **371** 658
[24] Zhang L, Yue H, Li M, Wang S and Mi X Y 2015 *Acta Phys. Sin.* **64** 060505 (in Chinese)
[25] Dong H R, Meng Q, Yao X M, Yang X X and Wang Q L 2017 *Chin. Phys. B* **26** 098902
[26] Yue H, Shao C F and Yao Z S 2009 *Acta Phys. Sin.* **58** 4523 (in Chinese)
[27] Yue H, Shao C F, Guan H Z and Duan L M 2010 *Acta Phys. Sin.* **59** 4499 (in Chinese)
[28] Yue H, Zhang X, Chen G and Shao C F 2012 *Acta Phys. Sin.* **61** 130509 (in Chinese)
[29] Yue H, Zhang B Y, Shao C F and Xing Y 2014 *Chin. Phys. B* **23** 050512
[30] Blue V J and Adler J L 1998 *Transp. Res. Rec.* **1644** 29
[31] Blue V J and Adler J L 2001 *Transp. Res. Part. B* **35** 293
[32] Weng W G, Chen T, Yuan H Y and Fan W C 2006 *Phys. Rev. E* **74** 036102
[33] Sun Z, Jia B and Li X 2012 *Acta Phys. Sin.* **61** 100508 (in Chinese)

[34] Li X and Dong L Y 2012 *Chin. Phys. Lett.* **29** 098902
[35] Lu L L, Ren G, Wang W and Wang Y 2014 *Chin. Phys. B* **23** 088901
[36] Wei J, Zhang H, Guo Y and Gu M 2015 *Phys. Lett. A* **379** 1081
[37] Gokce S and Kayacan O 2016 *Chin. Phys. B* **25** 010508
[38] Lam W H K, Lee J Y S and Chenung C Y 2002 *Transportation* **29** 169
[39] Lee J Y S, Tam M L and Lam W H K 2005 *Proceedings of the Eastern Asia Society for Transportation Studies* **5** 1337
[40] Lee J Y S and Lam W H K 2008 *Transp. Res. Part. A* **42** 1314
[41] Alhajyaseen W K M and Nakamura H 2009 *Transportation Research Board* 88*nd Annual Meeting* January 10–14 2009 Washington DC, USA
[42] Guo H, Gao Z, Yang X and Jiang X 2011 *Traffic Inj. Prev.* **12** 96
[43] Zeng W, Chen P, Nakamura H and Iryo-Asano M 2014 *Transp. Res. Part. C* **40** 143
[44] Jia H F, Li Y X, Yang L L and Zhou Y N 2016 *Discrete Dyn. Nat. Soc.* **2016** 5625286
[45] Schroeder B, Rouphail N and Emerson R 2006 *Transp. Res. Rec.* **1956** 94
[46] King M J and Soole D 2009 *Accid. Anal. Prev.* **41** 485
[47] Morris M R, Pedersen M J, Skinner R E, *et al.* 2010 *Highway Capacity Manual* 4th edn. (Washington DC: Transportation Research Board)
[48] Golani A and Damti H 2007 *Transp. Res. Rec.* **2002** 125